**Marquette University**
**e-Publications@Marquette**

8-1-2017

# Observation and Understanding of the Initial Unstable Electrical Contact Behaviors

Wanbin Ren
*Harbin Institute of Technology*

Nan Jiang
*Harbin Institute of Technology*

Cheng Chang
*Harbin Institute of Technology*

Shengjun Xue
*Harbin Institute of Technology*

Yu Chen
*Harbin Institute of Technology*

**See next page for additional authors**

**Authors**
Wanbin Ren, Nan Jiang, Cheng Chang, Shengjun Xue, Yu Chen, and Ronald A. Coutu Jr.

## *Electrical and Computer Engineering Faculty Research and Publications/College of Engineering*

## Contents

# Observation and Understanding of the Initial Unstable Electrical Contact Behaviors

## Wanbin Ren

School of Electrical Engineering and Automation, Harbin Institute of Technology, Harbin, China

## Nan Jiang

School of Electrical Engineering and Automation, Harbin Institute of Technology, Harbin, China

## Cheng Chang

School of Electrical Engineering and Automation, Harbin Institute of Technology, Harbin, China

## Shengjun Xue

School of Electrical Engineering and Automation, Harbin Institute of Technology, Harbin, China

## Yu Chen

School of Electrical Engineering and Automation, Harbin Institute of Technology, Harbin, China

## Ronald A. Coutu

Department of Electrical and Computer Engineering, Marquette University, Milwaukee, WI

## Abstract:

Reliable and long-lifetime electrical contact is a very important issue in the field of radio frequency microelectromechanical systems (MEMS) and in energy transmission applications. In this paper, the initial unstable electrical contact phenomena under the conditions of micro-newton-scale contact force and nanometer-scale contact gap have been experimentally observed. The repetitive contact bounces at nanoscale are confirmed by the measured instantaneous waveforms of contact force and contact voltage. Moreover, the corresponding physical model for describing the competition between the electrostatic force and the restoring force of the mobile contact is present. Then, the dynamic process of contact closure is explicitly calculated with the numerical method. Finally, the effects of spring rigidness and open voltage on the unstable electrical contact behaviors are investigated experimentally and theoretically. This paper highlights that in MEMS systems switch, minimal actuation velocity is required to prevent mechanical bounce and excessive wear.

## Introduction

Microelectromechanical systems (MEMS) relays and switches have numerous potential applications due to their high throughput, cost efficiency, small size, and high integration capability with electric circuits.[1–2,3] Remarkably, radio-frequency MEMS switches can provide lower insertion loss, higher signal stability, higher cutoff frequency, excellent isolation, and lower power consumption compared to the traditional solid-state switches.[4,5] However, MEMS switch reliability is a major area for improvement for large-volume commercial applications.[6–7,8,9,10] Most of these critical issues, related to reliability, are closely related to the physics of electrical contacts. Much of the underlying physics and experience

gained with conventional electrical switches is described in Holm's classic book.[11] Recent work on MEMS switches where simple hemisphere-on-flat systems are to simulate MEMS switch behavior, have shown that the Au-to-Au contact metal failure remains an important issue at the micrometer and nanometer scales.[12–13,14,15] Admittedly, macroscopic contact bounce phenomena inevitably occur during the contacts breaking. They are generally attributed to the mechanical reaction due to high force and high velocity applied to the mobile contact part during contact closure. Therefore, the corresponding contact surface adhesion and contact welding inflict severe damage to the electrical contact and the lifetime of MEMS switches.[8,9,15]

Contact bounces in MEMS switches have been observed and studied in.[16–17,18,19] These papers mainly focus on the issue of contact bounce suppression by modifying actuation signals. The challenge is to perform high-speed commutation with near-zero impact velocity to avoid bounces. However, electrostatic actuation is not linear and is a complex dynamic problem, so that the velocity of impact is difficult to control. The disadvantage of very slow-making velocity on such small devices and gaps has been reported, that is, the curious contact voltage fluctuation phenomena accompanied with nanoscale bounce height is observed using atomic force microscope-based experimental setup. Peschot et al.[20] stated that the contact voltage fluctuation is attributed to the competition between the electrostatic force and the restoring force of the flexible mobile contact. It is worth mentioning that the electrostatic force is not neglected particularly under the slow-making velocity.

In addition, with regard to electrical contact behavior in metal-to-metal microcontacts, the oscillation of contact resistance phenomena is also observed before the minimum contact force reached. To better understand the mechanism behind the instabilities of electrical conductance during the critical period, Qiu et al.[21,22] concluded that the thin contaminant films may play an important role in unstable contact behavior, and presented the trap-assisted electron tunneling mechanism for explaining the phenomena. It is possible that the different mechanical properties, elastic or rigid contact, are the reason for the inconsistent explanation. However, to the best of our knowledge, the detailed Au-to-Au electrical contact behaviors in the initial unstable contact stage, and further the critical influencing factors, remain largely unexamined.

The purpose of this paper is to observe the transient contact voltage and contact force waveforms of metal-to-metal contacts with gold coatings, and to identify the factors that influence the unstable electrical contact behavior. The gold coating has been the most widely used among the candidate contact material in MEMS switches because of its low resistivity and high oxidation resistance.

For this purpose, fundamental studies on the contact voltage fluctuations behavior were carried out using the devised contact measurement apparatus, with which we can directly measure the contact voltage and contact force while the piezoactuator moves forward. From this, the characteristic parameters of contact voltage oscillation were extracted, and the relevant factors including spring stiffness and open voltage were also discussed and compared to dynamic contact models. When the initial contact instability and contact bounce phenomena is fully understood and mitigated, many new excited applications will be possible. Based on this, the experimental scheme is critical for conducting fundamental contact physics work. Additionally, these experiments are valuable for real switch design and relative electrical contact failure analysis.

# Experimental Details

The test apparatus used in these experiments is described in detail in,[15] which contains a brief summary thereof. A schematic of the test apparatus is shown in Fig. 1.The horizontal actuation of the moving electrode is obtained by means of a precision slider that is pushed by a piezoelectric actuator (LTC2013-013, PiezoMotor AB, Sweden). The desired displacement of the moving electrode is controlled by the motor driver with position feedback loop, which is provided by the assembled grating ruler (RGH25F-5 nm, Renishaw, U.K.). The motor driver (PMD101, PiezoMotor AB, Sweden) receives the controlling instruction from the PC and offers closed-loop control for the piezo motor by reading the feedback position of the grating ruler, which has a displacement resolution of 5 nm and a sampling rate of 10 Hz. The microstepping number of five steps per second and the step length of 30 nm are configured for the piezoactuator, so the average making and breaking velocity is 150 nm/s. A PWA090 electronic, self-leveling vibration isolation system was used to provide a portable, lightweight, and low-profile vibration-control solution. The vertical transmissibility at 10 Hz is −27 dB (95.66%). In addition, we use the bell jar made by the polymethyl methacrylate sheet to avoid the interference of air noise.
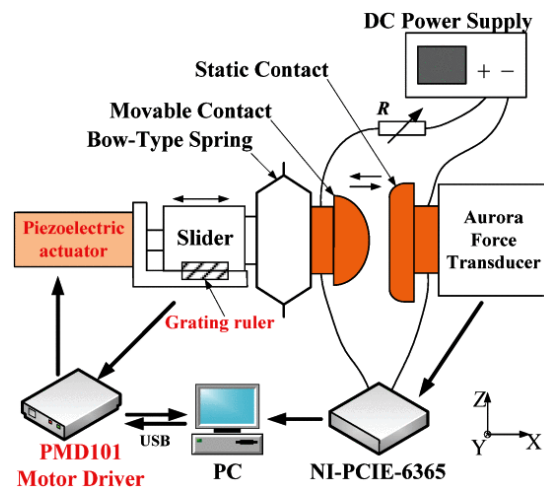


**Fig. 1.** Experimental circuit.

By using the four-wire method, the instantaneous value of contact voltage is continuously measured. The normal contact force between two electrodes is assessed using a force transducer (404A, Aurora Scientific, Canada), which has the measurement range of 100 mN and the resolution of 2 $\mu$N . During the test, the contact voltage and contact force are acquired by an acquisition board (PCIE6351, NI, USA) whose measuring range is ±10 V with the resolution of 16 b (0.3 mV) and the sampling rate of 1 kHz. The data of contact voltage and contact force could be uploaded to the PC simultaneously.

The electrodes are a hemisphere-shaped rider, with a diameter of 1.5 mm, on a flat sample, both made of a copper alloy structure and electroplated with gold (2 $\mu$m thick). In order to achieve the flexible contact with low force, the bow-type spring made from Beryllium bronze belt is introduced to connect with the movable contact. Hence, the structure is approximately equivalent to typical cantilever beams used in MEMS switches. The specimens are degreased using acetone, alcohol, and distilled water in an ultrasonic cleaner, dried, and carefully mounted in the test measurement apparatus. The experiments are carried out in ambient lab air. Table I shows the details of the experimental conditions.

**TABLE I** Experimental Conditions

| Parameters | Values |
|---|---|
| Open Voltage | 2V, 4V, 6V, 8V, 10V |
| Closed Current | 2mA |
| Piezoactuator Speed | 150nm/s |
| Bow-type spring stiffness | 22µN /µm, 56µN /µm, 100µN /µm |
| Environment Temperature | $20^0$C |
| Humidity | $38\pm2\%$ RH |

## Results and Discussion

### A. Initial Contact Behaviors During Contact Making

Fig. 2 shows an example of the measured variation in contact voltage, contact force, and piezoactuator position of Au-to-Au contacts as a function of time. The open voltage is 10 V, and the closed current is 2 mA. The velocity of the actuator movement is maintained at about 150 nm/s. The whole making process of contact can be typically divided into three regions, as illustrated in Fig. 2: I) a free travel region in which the contact voltage keeps high level and the contact force changes from zero into negative, and the maximum tension is about 2.5 $\mu$N ; II) an substantial unstable contact region with the oscillations of contact voltage between 10 V and 20 mV, combined with the cyclic change of contact force ($-6$ to 18 $\mu$N ), which is described in detail in Fig. 2; and III) finally, the relative stable contact region with the low-level contact voltage (no more than 8 mV) and the step-like increase of contact force.
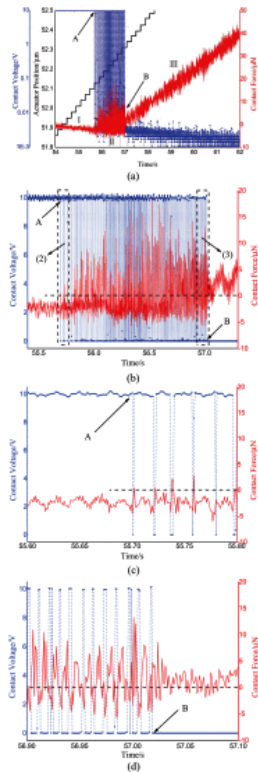


**Fig. 2.** Measured example of the variation of the contact voltage, contact force, and piezoactuator position as a function of the time (open voltage: 10 V; load current: 2 mA; breaking velocity: 150 nm/s; spring stiffness

56 $\mu N/\mu m$ ). (a) Whole process. (b) Zoom between point A and point B. (c) Zoom of region (2). (d) Zoom of region (3).

Fig. 2(b)–(d) shows explicitly 2 and 0.2 s zoom of the contact voltage and the contact force waveforms in Fig. 2(a). It is noticed that in region II there is almost no contact voltage data distributed between 1 and 9 V. For simplicity, the contact voltage below 1 V is defined as the "ON" state while the voltage above 9 V is taken as "OFF" state. Therefore, the contact voltage fluctuation behavior could be described as the contact state alternating between "ON" and "OFF" periodically. Examination of Fig. 2(c) and (d) reveals that the dropping movement of the contact voltage corresponds exactly with the contact force substantially shifting to the positive of 2 $\mu N$ , while the restored open voltage is consistent well with the negative contact force of 5 $\mu N$ . The situation of contact force indicates that the contact bounce phenomena occurred. The whole contact bounce duration is about 1.3 s, and the bounce happens 99 times. Initially, the bounce cycle is about 20 ms, and the "OFF" state occupies 90% of one cycle. However, the bounce cycle decreases to 11 ms, and the "OFF" state is only about 3 ms in the end. The signal noise is mainly attributed to the measurement circuit and the input wall power. The maximum noise of force signal channel is about 3.5 $\mu N$ , which can be read from the corresponding waveform from 55.6 to 55.7 s in Fig. 2(c). The contact voltage signal noise is no more than 5 mV.

## B. Physical Mechanism of Initial Unstable Electrical Contact

The oscillation of contact voltage and contact force, which is observed in the unstable contact Region II, indicates that the continuous impact and bounce of gold contacts occur repeatedly. The initial oscillation distance of 150 nm could be estimated by the product of the contact bounce duration of 1 s and the motion velocity of 150 nm/s. According to the classical impact theory, such very slow velocity of movable contact could not induce the bounce behavior. However, as shown in Fig. 3, the electrostatic force is preponderant, and the attractive properties have to be considered at the nanometer scale.
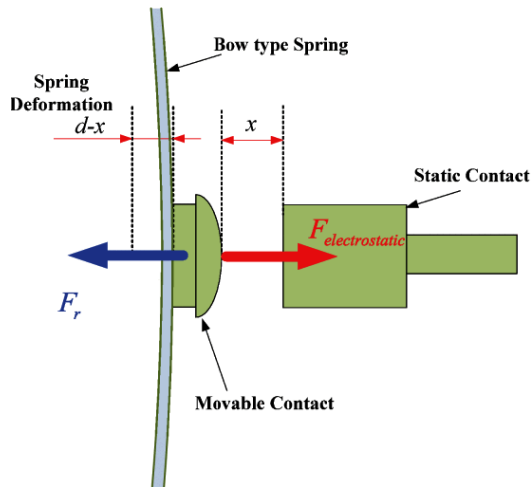


**Fig. 3.** Illustration of forces acting on the contacts.

The electrostatic force $F$electrostatic is described as

$$F\text{electrostatic}(x)=\frac{\epsilon_0 S U^2}{2x^2}$$

where $\varepsilon_0$ is the permittivity; $S$ depends on the surface of contact; $U$ is the potential across the contact; and $x$ is the gap distance between two contacts.

The only repulsive force is the restoring force of the bow-type spring. It is the sole force to open a contact. The restoring force $Fr$ depends on the stiffness of the spring $k$, the deformation of the spring $(d-x)$, in which $d$ is the contact gap without the spring deformation. It can be simply described by the relation

$F_r$ (x, d) = k(d-x)

As the surface area of contact could not be measured directly, then we assume $S=100$ $\mu m2$, and $d=300$ nm or $d=175$ nm, combined with the known $k=56$ $\mu N/\mu m$, $U=10$ V, and calculate the variations in electrostatic force and restoring force as a function of contact gap distance. As shown in Fig. 4, it is possible to observe that these two forces compete at small contact gaps, around a few hundreds of nanometers. $A$ is the equilibrium position of the electrostatic force and the restoring force. The force is only 0.53 $\mu N$, and the deformation of spring is 0.01 $\mu m$. Fig. 5(a) illustrates the initial equilibrium status.
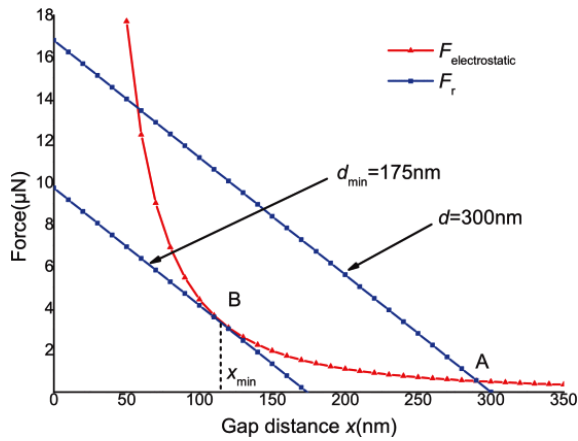


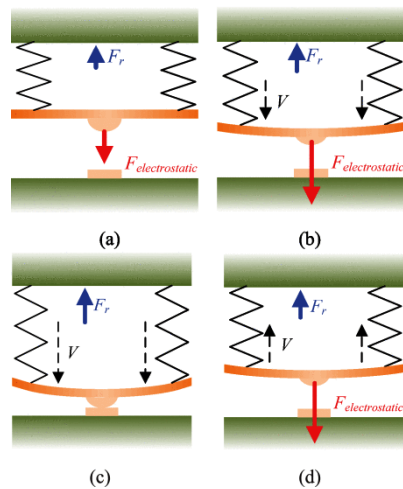**Fig. 4.** Attractive force and repulsive force before contact.



**Fig. 5.** Schematic showing the position of the movable contact in six distinct instants of the single bouncing process. (a) Initial equilibrium status. (b) Contact is moving toward the static electrode upon actuation of

electrostatic force. (c) Contact between electrodes and the bow-type spring is slightly bent, meanwhile the electrostatic force disappears. (d) Spring brings the movable contact rebound toward the starting noncontacting position while the electrostatic force recurs.

The piezoactuator motion causes the contact gap distance to be reduced, that is the decline of the $Fr - x$ curve. When $d\mathrm{min}$ is 175 nm, then the contact gap distance $x\mathrm{min}$ decreases to 117 nm, which is the threshold value of contact oscillation. As shown in Fig. 5(b), with the further reduced gap distance, the electrostatic force is always higher than the restoring force, and the movable contact is accelerated until closed, as shown in Fig. 5(c). Afterwards, the voltage across the two contact parts rapidly decreases down to nearly zero, so does the electrostatic force. The restoring force of the spring is maximum and competes with the adhesion force, which is produced by the Joule heat during contact make [23]. Once the restoring force exceeds over the surface adhesion, the contact bounce occurs and the electrostatic force reappears, as shown in Fig. 5(d), whereas the electrical contact builds up steadily. Since the deformation of spring is decreased during the contact approaching gradually, the provided restoring force is reduced correspondingly. That causes the "ON" state of contact to be extended and the "OFF" state shortened. Therefore, the cycle of contact bounce during the making process and the duty ratio decrease gradually. Hence, we define $x\mathrm{min}$ as the threshold distance of the contact voltage fluctuation. This position satisfies

$$F_{electrostatic}(x) = F_r(x)$$

and

$$\frac{F_{electrostatic}(x)}{dx} = \frac{F_r(x)}{dx}$$

Substitute (1) and (2) into (3) and (4)

$$x_{min} = \sqrt[3]{\frac{\epsilon_0 S U^2}{k}}$$

and then $d_{min} = 1.5 x_{min}$ .

In order to study the transient behavior of tested contact pairs and relevant heavily influencing factors, the lumped model and typical behavior for a generic spring oscillator are shown in Fig. 5, and its dynamics in "OFF" state can be modeled as

$$m\frac{d^2x}{dt^2} = \frac{\epsilon_0 S U^2}{k} - k(d - x)$$

where $m$ is the equivalent mass of 0.657 g, which is equal to the movable contact and half of bow-type spring. Assume the piezoactuator moves forward a microstep of 30 nm, then $d* = d_{min} - 30$ nm $= 145$ nm, combined with the initial velocity of movable contact $v_0 = 0$ and $x_0 = x_{min} = 23 d_{min} \approx 117$ nm, the step length $\Delta t = 1 \, \mu s$ , so the recurrence formula with the use of forward Euler method is given by

$$F_i = \frac{\epsilon_0 S U^2}{2x_i^2} - k(d^* - x_i)$$

$$v_{i+1} = v_1 + \frac{F_i}{m}\Delta t$$

$$x_{i+1} = x_1 - v_1 \Delta t$$

The variations in resultant force $F_i(t)$ , gap distance $x_i(t)$ , and velocity $v_i(t)$ in relation to the first closure of contact are shown in Fig. 6. Thus, the corresponding close time $t_{close}$=7.6 ms.
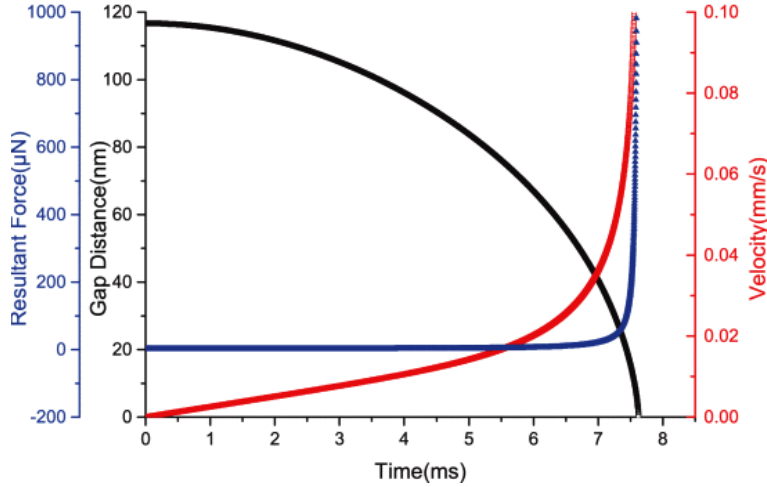


**Fig. 6.** Calculated transient resultant force, gap distance, and velocity of movable contact with known initial gap distance.

The "ON" state corresponds to the impact of contact and the kinetic energy converting to the elastic potential energy. The repulsive force decreases gradually in the subsequent bounce process, therefore $t_{ON}$ has the increase trend during the pull-in process. The calculation of $t_{ON}$ is challengeable. Assuming the energy dissipation during impact is neglected, and the open time $t_{open}$ is equal to the close time $t_{close}$ , then the "OFF"-state duration $t_{OFF}$ is 15.2 ms. The detailed definition of associated time parameters during the continuous contact bounce is shown in Fig. 7.
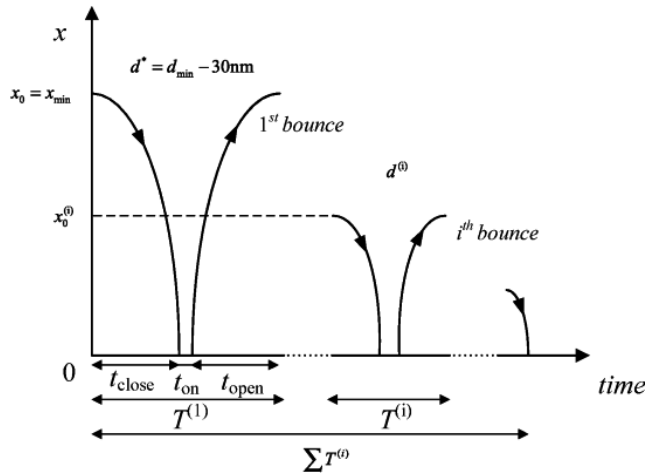


**Fig. 7.** Definition of associated time parameters during the continuous contact bounce.

With the help of <u>(7)–(9)</u>, for a given initial contact gap $d(i)=d*-i \cdot$ step, step =10 nm, $x_0(i)=d(i)$ , then the relationship between "OFF"-state duration $t$OFF and contact gap could be calculated accurately

(shown in Fig. 8). Therefore, the threshold distance of the contact voltage fluctuation $x_{min}$ is 92, 117, 147, and 168 nm with varied contact area, and the corresponding $t$OFF is 15.4, 17.2, 19.2, and 19.8 ms. When the open voltage is changed as 10, 8, and 6 V, the threshold distance $x_{min}$ is 117, 100, and 83 nm, while the corresponding $t$OFF is 17.2, 16.1, and 14.5 ms. In the case of the spring stiffness $k$ of 100, 56, and 22 $\mu N/\mu m$ , the threshold distance $x_{min}$ is 96, 117, and 159 nm, while the corresponding $t$OFF is 11.9, 17.2, and 31.2 ms. This suggests that the increase of contact area and open voltage lengthen the threshold distance of contact bounce and corresponded contact closing duration by comparisons. Also, the change rates of $x$min and $t$OFF reduce gradually with the decrease of contact gap, while they are negligible for the varied spring stiffness. That is to say, when higher open voltage or softer spring is exposed on the contact pairs, it will result in the occurrence of contact bounce in advance under such slow velocity.
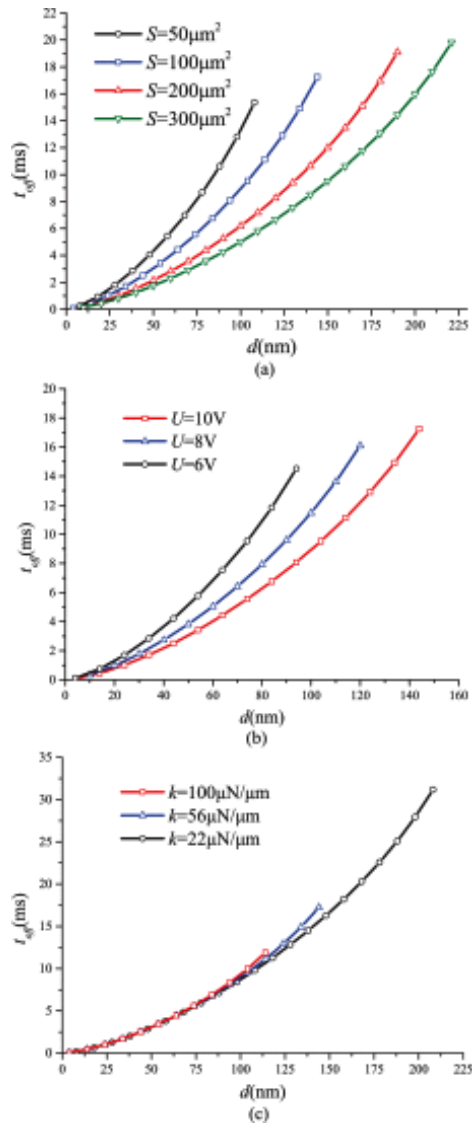


**Fig. 8.** Relationship between $t_{OFF}$ and gap distance with different influencing factors. (a) Surface of contact (open voltage 8 V and spring stiffness 56 $\mu N/\mu m$ ). (b) Open voltage (surface of contact 100 $\mu m^2$ and spring stiffness 56 $\mu N/\mu m$ ). (c) Spring stiffness (surface of contact 100 $\mu m^2$ and open voltage 8 V).

We collected three distinct time parameters $t$ON , $t$OFF , and $T$ within the consecutive contact bounce process, and the corresponding linear fitting relationships between such time parameters and actuation time are shown in Fig. 9. As seen, the contact bounce cycle $T$ decreases monotonously from 18 to 10 ms, $t$OFF reduces from 15 to 2 ms, and $t$ON increases significantly from 3 to 8 ms. Thus, the ratio of $t$ON /T to these individual contact bounces rises largely from 17% to 80%, and the total contact bounce number is 99 times. It indicates that there are such monotonous variations of time parameters related to contact voltage.
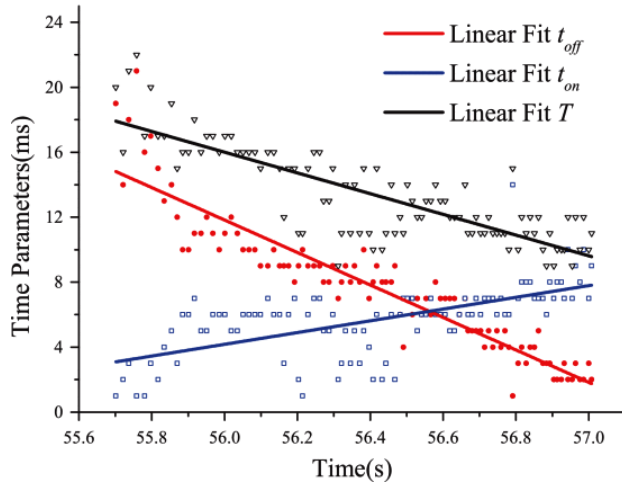


**Fig. 9.** Collected time parameters of $t$ON , $t$OFF , and $T$ within the consecutive contact bounce process (the original waveform of contact voltage is shown in Fig. 2).

## C. Experimental Validation of Influencing Factors

To validate above theoretical analysis and discussion, we further experimentally investigated effects of spring stiffness and open voltage on critical contact gap distance and relevant time parameters. First, the spring stiffness is taken as one variable, which is 22, 56, and 100 $\mu$N/$\mu$m individually, and the open voltage is 10 V, current is 20 $\mu$A , and the actuator velocity is 150 nm/s. As shown in Fig. 10(a), the contact bounce cycle $Ti$ and the whole bounce duration increase obviously with the reduced spring stiffness. Meanwhile, the collected $T$OFF time parameter also has the similar trend with the proceeding contact bounces. The whole contact bounce duration increases from 0.8 to 1 and 1.4 s. However, the spring stiffness has not such an obvious monotonous effect on the $t$ON time parameter. According to the principle of structural dynamics, the contact bounce cycle is mainly determined by the bow-type spring stiffness and equivalent mass. Furthermore, the $t$ON time parameter also correlates with contact impact and friction.
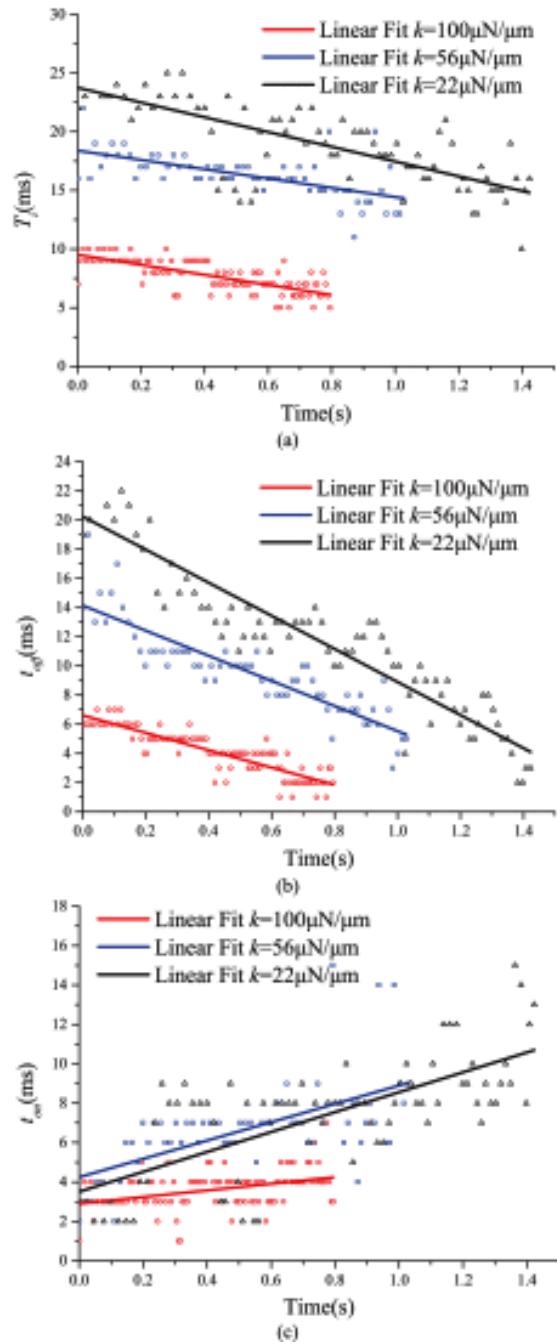
**Fig. 10.** Effect of spring stiffness on contact bouncestime parameters. (a) Variations in contact bounce cycle $T_i$. (b) Variations in "OFF" time for each contact bounce cycle $t_{OFF}$. (c) Variations in "ON" time for each contact bounce cycle $t_{ON}$.

Second, the open voltage is taken as the other variable, which is 10, 8, 6, and 2 V individually, and the spring stiffness is 56 $\mu N/\mu m$, current is 20 $\mu A$, and the actuator velocity is 150 nm/s. As shown in Fig. 11(a), the contact bounce cycle $Ti$ and the whole bounce duration increase obviously with the increase of open voltage. That is attributed to the increase of the electrostatic force, which is determined by the open voltage directly. However, the electrostatic force has no relation with the spring deformation, so $t$ON time parameter does not correlate with the excited voltage. The results of critical contact bounce

gap distance obtained from experiments agree well with that of theoretical formula, so as to the $t$OFF time parameter. It proves that the whole contact bounce analysis is reasonable.
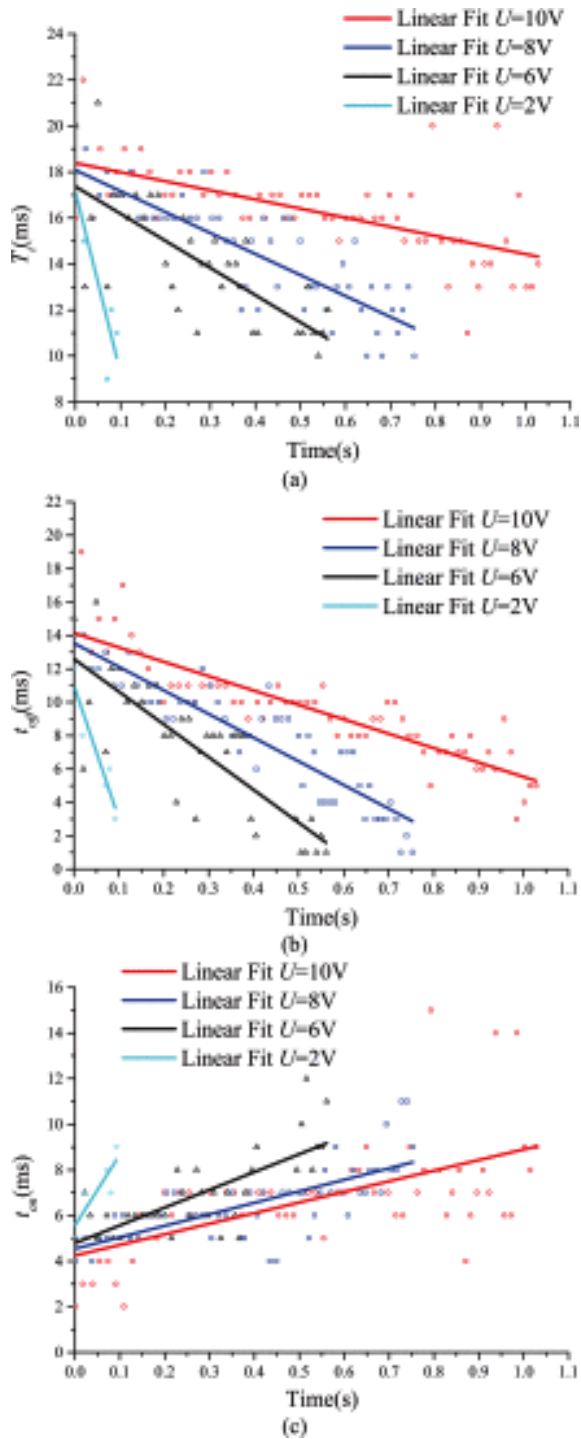


Fig. 11. Effect of open voltage on contact bounces time parameters. (a) Variations in contact bounce cycle $T_i$. (b) Variations in "OFF" time for each contact bounce cycle $t_{OFF}$. (c) Variations in "ON" time for each contact bounce cycle $t_{ON}$.

## Conclusion

This paper describes the complexity of initial unstable electrical contact under low velocity of 150 nm/s and hot switching conditions (2–10 V/20 $\mu A$ ). Recorded explicit contact voltage and contact force waveforms together demonstrate the presence of contact bounce in nanometer scale. The fundamental mechanism for the instability of electrical conductance at the microsecond scale can explain the competition between electrostatic force and spring repulsive force. It is noted that surface forces can lead to multiple bounces when the contact gap is reduced to several tens of nanometers. Moreover, the consecutive contact bounce is equivalent to generic spring oscillator with decreased bounce cycle. Meanwhile, the "OFF"-state time parameter also tends to decrease with the contact pair approaching. Spring stiffness and open voltage are main influencing factors of the initial unstable electrical contact behaviors.

## References

**1.** G. M. Rebeiz, J. B. Muldavin, "RF MEMS switches and switch circuits", *IEEE Microw. Mag.*, vol. 2, no. 4, pp. 59-71, Dec. 2001.

**2.** G. M. Rebeiz, RF MEMS: Theory Design and Technology, Hoboken, NJ, USA:Wiley, 2003.

**3.** M. Esashi, T. Ono, "From MEMS to nanomachine", *J. Phys. D Appl. Phys.*, vol. 38, no. 13, pp. R223, 2005.

**4.** R. Stefanini, M. Chatras, P. Blondy, G. M. Rebeiz, "Miniature MEMS switches for RF applications", *J. Microelectromech. Syst.*, vol. 20, pp. 1324-1335, Dec. 2011.

**5.** R. Plana, "What's hot in RF components and systems", *Microw. J.*, vol. 49, no. 2, pp. 22-28, Feb. 2006.

**6.** D. Hyman, M. Mehregany, "Contact physics of gold microcontacts for MEMS switches", *IEEE Trans. Compon. Packag. Technol.*, vol. 22, no. 3, pp. 357-364, Sep. 1999.

**7.** B. F. Toler, R. A. Coutu, J. W. McBride, "A review of micro-contact physics for microelectromechanical systems (MEMS) metal contact switches", *J. Micromech. Microeng.*, vol. 23, no. 10, pp. 103001, 2013.

**8.** A. Basu, R. P. Hennessy, G. G. Adams, N. E. McGruer, "Hot switching damage mechanisms in MEMS contacts—Evidence and understanding", *J. Micromech. Microeng.*, vol. 24, no. 10, pp. 105004, 2014.

**9.** T. Ishida, K. Kakushima, H. Fujita, "Degradation mechanisms of contact point during switching operation of MEMS switch", *J. Microelectromech. Syst.*, vol. 22, no. 4, pp. 828-834, Aug. 2013.

**10.** A. Tazzoli, M. Barbato, F. Mattiuzzo, V. Ritrovato, G. Meneghesso, "Study of the actuation speed bounces occurrences and contact reliability of ohmic RF-MEMS switches", *Microelectron. Rel.*, vol. 50, pp. 1604-1608, Sep./Nov. 2010.

**11.** R. Holm, Electric Contacts: Theory and Application, Berlin, Germany:Springer, 1967.

**12.** H. Kwon et al., "Investigation of the electrical contact behaviors in Au-to-Au thin-film contacts for RF MEMS switches", *J. Micromech. Microeng.*, vol. 18, no. 10, pp. 105010, 2008.

**13.** S. T. Patton, J. S. Zabinski, "Fundamental studies of Au contacts in MEMS RF switches", *Tribol. Lett.*, vol. 18, no. 2, pp. 215-230, 2005.

**14.** G. Gregori, D. R. Clarke, "The interrelation between adhesion contact creep and roughness on the life of gold contacts in radio-frequency microswitches", *J. Appl. Phys.*, vol. 100, no. 9, pp. 094904, 2006.

**15.** W. Ren, C. Chang, Y. Chen, S. Xue, R. A. Coutu, "Investigation of the surface adhesion phenomena and mechanism of gold-plated contacts at superlow making/breaking speed", *IEEE Trans. Compon. Packag. Manuf. Technol.*, vol. 5, no. 6, pp. 771-778, Jun. 2015.

**16.** D. A. Czaplewski, "A soft-landing waveform for actuation of a single-pole single-throw ohmic RF MEMS switch", *J. Microelectromech. Syst.*, vol. 15, no. 6, pp. 1586-1594, Dec. 2006.

**17.** H. Sumali, J. E. Massad, D. A. Czaplewski, C. W. Dyck, "Waveform design for pulse-and-hold electrostatic actuation in MEMS", *Sens. Actuators A Phys.*, vol. 134, pp. 213-220, Feb. 2007.

**18.** Z. J. Guo, N. E. McGruer, G. G. Adams, "Modeling simulation and measurement of the dynamic performance of an ohmic contact electrostatically actuated RF MEMS switch", *J. Micromech. Microeng.*, vol. 17, no. 9, pp. 1899-1909, Aug. 2007.

**19.** J. C. Blecke, "A simple learning control to eliminate RF-MEMS switch bounce", *J. Microelectromech. Syst.*, vol. 18, no. 2, pp. 458-465, Apr. 2009.

**20.** A. Peschot, C. Poulain, N. Bonifaci, O. Lesaint, "Contact bounce phenomena in a MEM switch", *Proc. 58th IEEE Holm Conf. Electr. Contacts*, pp. 49-55, Sep. 2012.

**21.** H. Qiu, H. Wang, F. Ke, "Understanding of initial unstable contact behaviors of Au-to-Au microcontact under low contact force for microand nano-electromechanical system devices", *Jpn. J. Appl. Phys.*, vol. 52, no. 9R, pp. 090203, 2013.

**22.** H. Qiu, H. Wang, F. Ke, "Instability of contact resistance in MEMS and NEMS DC switches under low force: The role of alien films on the contact surface", *Sensors*, vol. 13, no. 2, pp. 16360-16371, 2013.

**23.** W. Ren, S. Xue, H. Zhi, G. Zhai, "Preliminary study of electrical contact behaviors of Au-plated material at super low making/breaking velocity", *IEICE Trans. Electron.*, vol. E98-C, no. 4, pp. 364-370, 2015.